



Measurements of CP violation in multibody charm decays

Denis Derkach

on behalf of the LHCb collaboration

University of Oxford, Keble road, Oxford, OX1 3RH, United Kingdom

Abstract

Charmed hadrons are a unique probe of CP violation with up-type quarks. Yet, CP violation in the charm sector is very suppressed by tiny CKM phases in the Standard Model. Any large non-zero measurement would thus be a sign of New Physics. We report on recent measurements of CP asymmetries in multibody charmed meson and baryon decays. The CP asymmetries are studied in regions of the Dalitz space.

Keywords: CP violation, Charm physics, CKM matrix

1. Introduction

The Standard model of elementary particles (SM) describes mixing using a single Cabibbo-Kobayashi-Maskawa (CKM) matrix. In the framework of the SM, charge-parity (CP) violation in the charm sector is expected to be small. Quantitative predictions of CP asymmetries are difficult, since the computation of strong-interaction effects in the non-perturbative regime is involved and long distance effects have to be considered. In spite of this, it was commonly assumed that the observation of asymmetries of the order of 1% in charm decays would be an indication of new sources of CP violation [1, 2, 3, 4].

Experimentally, the sensitivity for CP violation searches has substantially increased with the advent of the large LHCb data set. CP asymmetries at the $O(10^{-2})$ level are now disfavoured. With uncertainties approaching $O(10^{-3})$, the current CP violation searches start to probe the regime of SM expectations. Certain extensions to the SM predict an increase of up to an order of magnitude in penguin contributions in charm decays.

The simplest and most direct technique for CP violation searches is the computation of an asymmetry between the time-integrated particle and anti-particle decay rates. A single number, however, may not be sufficient for a comprehension of the nature of the CP vio-

lating asymmetry. In this context, three- and four-body decays benefit from rich resonance structures with interfering amplitudes modulated by strong-phase variations across the phase space. Searches for localised asymmetries can bring complementary information on the nature of the CP violation.

Direct CP violation can occur through interferences between penguin and tree level contributions. For this reason, we use the Singly-Cabbibo Suppressed (SCS) decays, $D^+ \rightarrow \pi^+\pi^-\pi^+$, $D^0 \rightarrow \pi^+\pi^-\pi^+\pi^+$, and $D^0 \rightarrow K^+K^-\pi^+\pi^-$, where both penguin and tree level processes contribute. In the analyses presented, we use two model-independent methods: binned and unbinned.

We reconstruct three- and four- body decays and analyse them using model-independent methods. The $D^+ \rightarrow \pi^-\pi^+\pi^+$ ¹ channel, which is a self-tagged, is reconstructed as is, while the D^0 , giving a 4-body final state ($\pi^+\pi^+\pi^-\pi^-$ or $K^+\pi^+K^-\pi^-$) has to have an additional tag. Thus the $D^{*+} \rightarrow D^0\pi^+$ decay is reconstructed to obtain an initial flavour of D^0 . We also reconstruct $D_s^+ \rightarrow \pi^-\pi^+\pi^+$ and $D^0 \rightarrow K^+\pi^+\pi^-\pi^-$ as control channels, where CP violation is expected to be negligible. Additional information on the analyses can be found

¹Unless stated explicitly, the inclusion of charge conjugate states is implied.

in [5] and [6]. The LHCb detector is described in detail elsewhere [7].

2. Selection

To reduce the combinatorial background when reconstructing charged and neutral D mesons, requirements on the quality of the reconstructed tracks, their χ_{IP}^2 , p_{T} , and scalar p_{T} sum are applied. Additional requirements are made on the secondary vertex fit quality, the minimum significance of the displacement from the secondary to any primary vertex in the event, and the χ_{IP}^2 of the $D_{(s)}^+$ candidate (if it exists in the reconstructed decay). This also reduces the contribution of secondary D mesons from b -hadron decays to 1–2%, avoiding the introduction of new sources of asymmetries. The final-state particles are required to satisfy particle identification (PID) criteria based on the RICH detectors. We also apply a muon veto in order to avoid the contribution of semileptonic D meson decays. The D^{*+} candidates are reconstructed from D^0 candidates combined with a track with high transverse momentum.

The next step is to obtain the signal yields and CP violation sensitivity. For the 3-body channel, this is done using the 1 dimensional fits to the invariant mass distribution $M(\pi^-\pi^+\pi^+)$. These fits are performed for the D^+ and D_s^+ candidates satisfying the above selection criteria and within the range $1810 < M(\pi^-\pi^+\pi^+) < 1930 \text{ MeV}/c^2$ and $1910 < M(\pi^-\pi^+\pi^+) < 2030 \text{ MeV}/c^2$, respectively. The signal is described by a sum of two Gaussian functions and the background is represented by a third-order polynomial. The data sample is separated according to magnet polarity and candidate momentum ($p_{D_{(s)}^+} < 50 \text{ GeV}/c$, $50 < p_{D_{(s)}^+} < 100 \text{ GeV}/c$, and $p_{D_{(s)}^+} > 100 \text{ GeV}/c$), to take into account the dependence of the mass resolution on the momentum. The parameters are determined by simultaneous fits to these $D_{(s)}^+$ and $D_{(s)}^-$ subsamples. The results of the fits are shown in Figure 1.

In the case of 4-body decays, we exploit the reconstructed D^{*+} and construct a specific parameter ΔM , the difference in the reconstructed D^{*+} mass and D invariant mass, m_D , for candidate decays. Figure 2 shows the m_D and ΔM distributions for D^0 candidate decays to the $K^+K^-\pi^+\pi^-$ final state with fit overlaid. The signal distribution is described by a Johnson function [8] in ΔM and a Crystal Ball function [9] plus a Gaussian function, with a shared peak value, in m_D . The combinatorial background is modeled with a first-order polynomial in m_D , and the background from D^0 candidates each associated with a random soft pion is modeled by a Gaussian distribution in m_D . Both combinatorial and

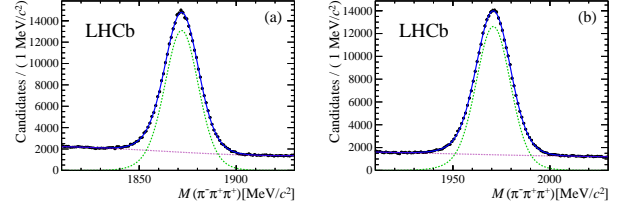


Figure 1: Invariant-mass distributions for (a) D^+ and (b) D_s^+ candidates in the momentum range $50 < p_{D_{(s)}^+} < 100 \text{ GeV}/c$ for magnet up data. Data points are shown in black. The solid (blue) line is the fit function, the (green) dashed line is the signal component and the (magenta) dotted line is the background.

random soft pion backgrounds are modeled with a function of the form

$$f(\Delta M) = \left[(\Delta M - \Delta M_0) + p_1 (\Delta M - \Delta M_0)^2 \right]^a \quad (1)$$

in ΔM , where ΔM_0 is the kinematic threshold (fixed to the pion mass), and the parameters p_1 and a are allowed to float. Partially reconstructed decays are investigated with simulated events.

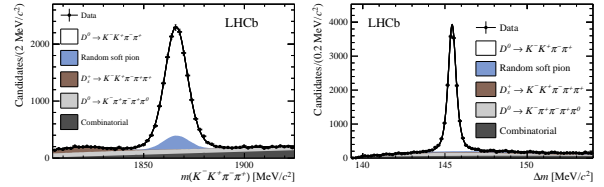


Figure 2: Distributions of m_D and ΔM for D^0 candidate decays to the $K^+K^-\pi^+\pi^-$. Data points are shown in black.

The obtained yields are shown in Table 1. These yields are then taken into account when estimating the sensitivities of methods.

Table 1: Yields for relevant channels.

Decays	Signal Yield, 10^3
$D^+ \rightarrow \pi^+\pi^-\pi^+$	2678 ± 7
$D_s^+ \rightarrow \pi^+\pi^-\pi^+$	2704 ± 8
$D^0 \rightarrow \pi^+\pi^-\pi^+\pi^-$	330
$D^0 \rightarrow K^+K^-\pi^+\pi^-$	57
$D^0 \rightarrow K^+\pi^-\pi^+\pi^-$	2900

3. Model Independent Binned Method

The binned method used to search for localised asymmetries in the D meson decay phase space is based on a bin-by-bin comparison between the D and \bar{D} Dalitz plots [10, 11]. For each bin of the Dalitz plot, the significance of the difference between the number of D and \bar{D} candidates, S_{CP}^i , is computed as

$$S_{CP}^i = \frac{N_i(D) - \alpha N_i(\bar{D})}{\sqrt{\alpha^2(\sigma^2(D) + \sigma^2(\bar{D}))}}, \quad \alpha = \frac{N(D)}{N(\bar{D})} \quad (2)$$

where $N_i(D)$ ($N_i(\bar{D})$) is the number of D (\bar{D}) candidates in the i -th bin and $N(D)$ ($N(\bar{D})$) is the sum of $N_i(D)$ ($N_i(\bar{D})$) over all bins; $\sigma_i(D)$ ($\sigma_i(\bar{D})$) is the associated uncertainty in the number of signal decays in bin i . The parameter α removes the contribution of global asymmetries which may arise due to production and detection asymmetries, as well as from CP violation. Two binning schemes are used, a uniform grid with bins of equal size and an adaptive binning where the bins have the same population.

In the absence of localised asymmetries, the S_{CP}^i values follow a Gaussian distribution. Therefore, CP violation can be detected as a deviation from this behaviour. The comparison between the D and \bar{D} Dalitz plots is made using a χ^2 test, with $\chi^2 = \sum_i (S_{CP}^i)^2$. A p-value for the hypothesis of no CP violation is obtained considering that the number of degrees of freedom (ndf) is equal to the total number of bins minus one, due to the constraint on the overall D/\bar{D} normalisation.

A CP violation signal is established if a p-value lower than 3×10^{-7} is found. If no evidence of CP violation is found, this technique provides no model-independent way to set an upper limit.

To study the CP violation sensitivity of the method for the current data set, a number of simulated pseudo-experiments are performed with sample size and purity similar to that observed in data. The generated experiments followed the most up-to-date model of the corresponding decay [12, 13, 14]. The study shows a sensitivity (p-values below 10^{-7}) around 1° to 2° in phase differences and 2% in amplitude in 3-body channels and a phase difference of 10° or a magnitude difference of 10% for 4-body decays. The sensitivity for different binning strategies is also evaluated.

The p-values are found to be within 0.4–95.5%, consistent with differences in the number of D^+ and D^- candidates arising from statistical fluctuations. Since the selection criteria suppress charm background decays to a negligible level, it is assumed that the background contribution to the signal is similar to the sidebands.

Therefore, asymmetries eventually observed in the signal mode cannot be attributed to the background. An example of resulting plots as well as Dalitz plane for 3-body decay can be found in Figures 3 and 4.

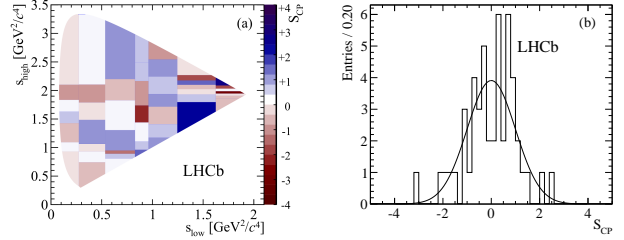


Figure 3: (a) Distribution of S_{CP}^i with 49 D_s^+ adaptive bins of equal population in the $D_s^+ \rightarrow \pi^+\pi^-\pi^+$ Dalitz plot and (b) the corresponding one-dimensional distribution (histogram) with a standard normal Gaussian function superimposed (solid line).

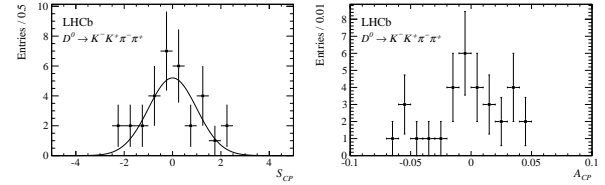


Figure 4: Distributions of (a) S_{CP}^i and (b) local CP asymmetry per bin for $D^+ \rightarrow K^+K^-\pi^+\pi^-$ decays partitioned with 32 bins. The points show the data distribution and the solid line is a reference Gaussian distribution corresponding to the no CP violation hypothesis.

4. Model Independent Unbinned Method

The unbinned model-independent method to search for CP violation in many-body decays uses the concept of nearest neighbour events. In the three-body decay, we also apply unbinned method to D and \bar{D} samples to test whether they share the same parent distribution function [15, 16, 17]. To find the n_k nearest neighbour events of each D and \bar{D} event, the Euclidean distance between points in the Dalitz plot of three-body D and \bar{D} decays is used. For the whole event sample a test statistic T for the null hypothesis is calculated,

$$T = \frac{1}{n_k(N_+ + N_-)} \sum_{i=1}^{N_++N_-} \sum_{k=1}^{n_k} I(i, k), \quad (3)$$

where $I(i, k) = 1$ if the i th event and its k th nearest neighbour have the same charge and $I(i, k) = 0$ otherwise and N_+ (N_-) is the number of events in the D (\bar{D}) sample.

The test statistic T is the mean fraction of like-charged neighbour pairs in the combined D and \bar{D} decays sample. The advantage of the k -nearest neighbour method (kNN), in comparison with other proposed methods for unbinned analyses [15], is that the calculation of T is simple and fast and the expected distribution of T is well known: for the null hypothesis it follows a Gaussian distribution with mean μ_T and variance σ_T^2 calculated from known parameters of the distributions,

$$\mu_T = \frac{N_+(N_+ - 1) + N_-(N_- - 1)}{N(N - 1)}, \quad (4)$$

$$\lim_{N, n_k, D \rightarrow \infty} \sigma_T^2 = \frac{1}{N n_k} \left(\frac{N_+ N_-}{N^2} + 4 \frac{N_+^2 N_-^2}{N^4} \right), \quad (5)$$

where $N = N_+ + N_-$ and D is a space dimension. For $N_+ = N_-$ a reference value

$$\mu_{TR} = \frac{1}{2} \left(\frac{N - 2}{N - 1} \right) \quad (6)$$

is obtained and for a very large number of events N , μ_T approaches 0.5. However, since the observed deviations of μ_T from μ_{TR} are sometimes tiny, it is necessary to calculate $\mu_T - \mu_{TR}$. The convergence in Eq. 5 is fast and σ_T can be obtained with a good approximation even for space dimension $D = 2$ for the current values of N_+ , N_- and n_k [15, 17].

The kNN method is applied to search for CP violation in a given region of the Dalitz plot in two ways: by looking at a “normalisation” asymmetry ($N_+ \neq N_-$ in a given region) using a pull $(\mu_T - \mu_{TR})/\Delta(\mu_T - \mu_{TR})$ variable, where the uncertainty on μ_T is $\Delta\mu_T$ and the uncertainty on μ_{TR} is $\Delta\mu_{TR}$, and looking for a “shape” or particle density function (pdf) asymmetry using another pull $(T - \mu_T)/\sigma_T$ variable. As in the binned method, this technique provides no model-independent way to set an upper limit if no CP violation is found.

The pull values of T and the corresponding p-values for the hypothesis of no CP violation are shown in Fig. 5 for the same regions. To check for any systematic effects, the test is repeated for samples separated according to magnet polarity. Since the sensitivity of the method increases with n_k , the analysis is repeated with $n_k = 500$ for all the regions. All p-values are above 20%, consistent with no CP asymmetry in the signal mode.

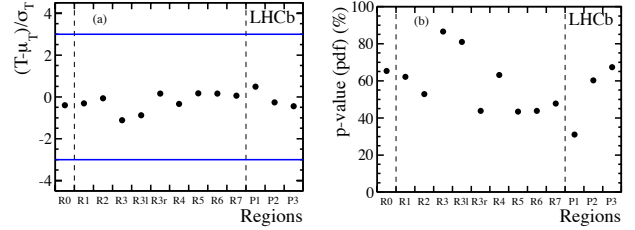


Figure 5: (a) Pull values of T and (b) the corresponding p-values for $D^+ \rightarrow \pi^+ \pi^- \pi^+$ candidates restricted to each region obtained using the kNN method with $n_k = 20$. The horizontal blue lines in (a) represent pull values -3 and $+3$. The region R0 corresponds to the full Dalitz plot. Note that the points for the overlapping regions are correlated.

5. Conclusions

A model-independent search for CP violation in $D^+ \rightarrow \pi^+ \pi^- \pi^+$, $D^0 \rightarrow \pi^+ \pi^- \pi^+ \pi^+$, and $D^0 \rightarrow K^+ K^- \pi^+ \pi^-$ decays is presented. The sensitivity in three-body case is around 1° to 2° in phase differences and 2% in amplitude for three body and of $O(10^\circ)$ or a magnitude difference of $O(10\%)$ for four-body cases. All channels give consistent results, compatible with no CP violation hypothesis.

Acknowledgements

We express our gratitude to our colleagues in the CERN accelerator departments for the excellent performance of the LHC. We thank the technical and administrative staff at the LHCb institutes. We acknowledge support from CERN and from the national agencies: CAPES, CNPq, FAPERJ and FINEP (Brazil); NSFC (China); CNRS/IN2P3 and Region Auvergne (France); BMBF, DFG, HGF and MPG (Germany); SFI (Ireland); INFN (Italy); FOM and NWO (The Netherlands); SCSR (Poland); MEN/IFA (Romania); MinES, Rosatom, RFBR and NRC “Kurchatov Institute” (Russia); MinECo, XuntaGal and GENCAT (Spain); SNSF and SER (Switzerland); NAS Ukraine (Ukraine); STFC (United Kingdom); NSF (USA). We also acknowledge the support received from the ERC under FP7. The Tier1 computing centres are supported by IN2P3 (France), KIT and BMBF (Germany), INFN (Italy), NWO and SURF (The Netherlands), PIC (Spain), GridPP (United Kingdom). We are thankful for the computing resources put at our disposal by Yandex LLC (Russia), as well as to the communities behind the multiple open source software packages that we depend on. The participant of the conference has received

funding from the People Programme (Marie Curie Actions) of the European Union's Seventh Framework Programme (FP7/2007-2013) under REA grant agreement n [329017].

References

- [1] J. Brod, Y. Grossman, A. L. Kagan and J. Zupan, *JHEP* **1210**, 161 (2012) [arXiv:1203.6659 [hep-ph]].
- [2] J. Brod, A. L. Kagan and J. Zupan, *Phys. Rev. D* **86** (2012) 014023 [arXiv:1111.5000 [hep-ph]].
- [3] B. Bhattacharya, M. Gronau and J. L. Rosner, *Phys. Rev. D* **85** (2012) 054014 [arXiv:1201.2351 [hep-ph]].
- [4] R. Aaij *et al.* [LHCb collaboration], *Eur. Phys. J. C* **73** (2013) 2373 [arXiv:1208.3355 [hep-ex]].
- [5] R. Aaij *et al.* [LHCb collaboration], *Phys. Lett. B* **728** (2014) 585 [arXiv:1310.7953 [hep-ex]].
- [6] R. Aaij *et al.* [LHCb collaboration], *Phys. Lett. B* **726** (2013) 623 [arXiv:1308.3189 [hep-ex]].
- [7] LHCb collaboration, A. A. Alves Jr. *et al.*, *JINST* **3** (2008) S08005.
- [8] N. L. Johnson, *Biometrika* **36** (1949) 149.
- [9] T. Skwarnicki, PhD thesis, Institute of Nuclear Physics, Krakow, 1986, DESY-F31-86-02.
- [10] I. Bediaga, I. I. Bigi, A. Gomes, G. Guerrer, J. Miranda and A. C. d. Reis, *Phys. Rev. D* **80** (2009) 096006 [arXiv:0905.4233 [hep-ph]].
- [11] B. Aubert *et al.* [BaBar collaboration], *Phys. Rev. D* **78** (2008) 051102 [arXiv:0802.4035 [hep-ex]].
- [12] E. M. Aitala *et al.* [E791 collaboration], *Phys. Rev. Lett.* **86** (2001) 770 [hep-ex/0007028].
- [13] M. Artuso *et al.* [CLEO collaboration], *Phys. Rev. D* **85** (2012) 122002 [arXiv:1201.5716 [hep-ex]].
- [14] J. M. Link *et al.* [FOCUS collaboration], *Phys. Rev. D* **75** (2007) 052003 [hep-ex/0701001].
- [15] M. Williams, *JINST* **5** (2010) P09004 [arXiv:1006.3019 [hep-ex]].
- [16] N. Henze, *The Annals of Statistics* **16** (1988) 772.
- [17] M. F. Schilling, *J. Am. Stat. Assoc.* **81** (1986) 799.